Table 5 Haplotype frequencies of two haplotype-tagging SNPs and their associations with the risk of arrhythmias

c.1673A>G (p.His558Arg) and c.5963T>G (p.Leu1988Arg)

	Selected locus		Haplotype frequency (%)			
Haplotype	c.1673A>G (p.His558Arg)	c.5963T>G (p.Leu1988Arg)	All subjects	Patients	Controls	Statistics
AT	A (His558)	T (Leu1988)	90.95	92.77	89.66	N.S.
GT	G (Arg558)	T (Leu1988)	7.54	6.93	7.97	N.S.
AG	A (His558)	G (Arg1988)	0.00	0.00	0.00	-
GG	G (Arg558)	G (Arg1988)	1.51	0.30	2.37	$p = 0.0181$
			Global permutation test[a]	$\chi^2 = 7.42$, $p = 0.0260$		

c.703+130G>A and c.4299 + 53T>C

	Selected locus		Haplotype frequency (%)		
Haplotype	c.703+130G>A	c.4299+53T>C	All subjects	Patients	Controls
GT	G	T	70.55	69.89	71.06
AT	A	T	2.32	3.60	1.35
GC	G	C	18.65	16.25	20.31
AC	A	C	8.49	10.25	7.27
			Global permutation test[a]	$\chi^2 = 8.64$, $p = 0.0550$	

[a]The empirical p values were obtained after 1000 permutations.

genetic variations in *SCN5A*. A total of 69 variations were detected in 166 unrelated Japanese arrhythmic patients and 232 healthy controls. Among them, 54 variations were novel and 15 were previously identified.

The fifteen reported variations include 4 nonsynonymous SNPs (p.His558Arg, p.Pro1090Leu, p.Arg1193Gln, and p.Val1951Leu). p.His558Arg has been extensively studied in various ethnic groups. Yang *et al.* (2002) have compared the frequency of p.His558Arg in patients diagnosed with the drug-associated LQT syndrome with those in three control populations: patients tolerating QT-prolonging drugs, and populations in Tennessee and accross the United States. p.His558Arg was detected at similar allele frequencies of 0.18–0.24 in all populations. As for the Japanese population, its frequencies were reported to be 0.132 for 56 healthy controls and 0.08 for 50 individuals by Takahata *et al.* (2003) and Iwasa *et al.* (2000), respectively. In our study, the allele frequency of p.His558Arg in arrhythmic patients (0.072) was slightly lower than that in the healthy controls (0.103), although a significant difference was not obtained ($p = 0.1307$). p.Pro1090Leu is a well-known nonsynonymous SNP localized in the linker between DII and DIII. The frequency of p.Pro1090Leu was 12/334 (0.036) and 11/464 (0.024) for the patients and the controls, respectively, and comparable to that reported in the Japanese (0.04) by Iwasa *et al.* (2000). Vatta *et al.* (2002) reported that p.Arg1193Gln accelerated the fast inactivation of the Na^+ channel *in vitro*. In our study, p.Arg1193Gln showed similar allele frequencies of 0.063 both in patients and healthy controls. From these results, it is likely that these three common SNPs are not directly involved in arrhythmogenesis in the Japanese. p.Val1951Leu, found at low frequencies in both patients (0.003) and healthy controls (0.004), was also detected at a similar frequency (0.005) by Iwasa *et al.* (2000). Although this SNP was reported in patients with BrS by Priori *et al.* (2002) and Mok *et al.* (2004), p.Val1951Leu alone is unlikely to be directly related with the pathogenesis of BrS.

Six novel nonsynonymous SNPs (p.Phe532Cys, p.Arg689His, p.Pro701Leu, p.His1200Tyr, p.Val 1667Ile, and p.Arg1739Gln) were found separately in six arrhythmic patients. When flanking amino acid sequences of these SNPs were aligned with related

sodium channel sequences (Supplementary Figure 1, online), the 6 amino acid residues of SCN5A, 532Phe, 689Arg, 701Pro, 1200His, 1667Val, and 1739Arg, were found top be highly conserved among the different Na^+ channel α subunit isoforms. Amino acid 532Phe, 689Arg, and 701Pro are localized in the linker between DI and DII, where the mutations associated with inherited arrhythmia syndrome such as p.Gly514Cys, p.Leu567Gln and p.Leu619Phe have already been reported (Tan *et al.* 2003). 1200His is located in the linker between DII and DIII, where the BrS-related variation p.Arg1193Gln (Vatta *et al.* 2002) is localized. 1667Val in DIVS5 and 1739Arg in the P loop of DIV form a pore structure together with DIVS6, where sodium channel blocking drugs are thought to bind. p.Arg1739Gln is a mutation located next to p.Gly1740Arg that was identified in a patient with BrS by Priori *et al.* (2002). Since these 4 novel nonsynonymous SNPs were not detected in 232 healthy controls, it is possible that they are related to cardiac arrhythmia pathogenesis, although these patients were not diagnosed with LQT or BrS. Some patients who carry these novel nonsynonymous SNPs simultaneously have p.His558Arg, p.Pro1090Leu or p.Val1951Leu (Table 3). At present it is not clear whether 1739Gln and 558Arg, 701Leu and 1951Leu or 1667Ile and 1090Leu are on the same chromosome. If they are, the interactions between the substituted residues may affect the biological properties of the Na^+ channels.

As for the five other novel nonsynonymous SNPs detected in healthy controls p.Glu428Lys is localized in the linker between DI and DII, p.Ala1148Thr and p.Ala1186Thr in the linker between DII and DIII, and p.Arg1913Cys and p.Ala1932Val in the C-terminal intracellular loop. 428Glu, 1148Ala and 1913Arg are well conserved, while 1186Ala and 1932Ala are not conserved (Supplementary Figure 1, online). Because the healthy individuals who carry these SNPs failed to show symptoms of arrhythmias, these SNPs are unlikely to affect Na^+ channel function. However, it has been recently suggested that some variations in *SCN5A* may increase the risk of acquired long QT syndrome triggered by drug administration in healthy individuals, who are clinically asymptomatic and have normal QT intervals under normal circumstances. Therefore, the possibility cannot be excluded that these five novel nonsynonymous SNPs in healthy controls influence the susceptibility to cardiac ion channel blockade and QT prolongation. We have begun analyzing the electrophysiological properties of the novel variations using heterologous expression systems. These studies will elucidate the importance of these variable sites in Na^+ channel function.

Another novel nonsynonymous SNP, p.Leu1988Arg, was heterozygous in eleven healthy subjects and one patient, and the allele frequency of p.Leu1988Arg was significantly lower in the patients than in the controls by Fisher's extract test ($p = 0.018$). Since all twelve subjects with p.Leu1988Arg also have p.His558Arg (Table 3), weak LD ($r^2 = 0.15$) was shown between p.His558Arg and p.Leu1988Arg (Figure 2). Haplotype analysis using the 2 SNPs, c.1673A>G (p.His558Arg) and c.5963T>G (p.Leu1988Arg), also showed that the frequency of the haplotype GG (558Arg–1988Arg) was significantly lower in the patients than in the healthy controls. These results suggest that the haplotype GG has been positively selected because of its protective effect against arrhythmias.

Although physiological characterization of Na^+ channels containing both p.His558Arg and p.Leu1988Arg are necessary to elucidate the negative association of the haplotype GG (558Arg-1988Arg) with cardiac arrhythmias, some underlying mechanisms could be speculated. 1988Leu is localized in the C-terminal intracellular loop but is not conserved among different Na^+ channel isoforms (Supplementary Figure 1, online). However, Cormier *et al.* (2002) reported that truncation of the distal region of the C-terminus (1921Leu stop mutant) reduced peak currents without affecting channel gating, by whole cell patch clamp recordings. Thus, it cannot be excluded that 1988Leu may be involved in regulating the density of functional Na^+ channels in the surface membrane. On the other hand, it has been postulated that p.His558Arg modulates functional changes of the Na^+ channel caused by other variations, and plays a role in intragenic complementation, although this common variation itself does not alter the voltage dependence of activation and inactivation kinetics of wild-type channels. For instance, Ye *et al.* (2003) showed that p.His558Arg restored the trafficking defect caused by the LQT-3 variation, p.Met1766Leu. Viswanathan *et al.* (2003) reported that p.His558Arg could attenuate

the abnormal gating effect caused by the proximal variation, p.Thr512Ile, *in vitro*. The favourable channel modulation by 1988Arg in conjunction with 558Arg for protection against arrhythmias might result in the positive selection of the GG (558Arg–1988Arg) haplotype in the controls. Alternatively, 558Arg could restore any functional deterioration caused by 1988Arg. If the intragenic complementation by 558Arg acts on 1988Arg, the rare frequency of the AG (558His–1988Arg) haplotype, and the preference of the GG (558Arg–1988Arg) haplotype, in the controls is reasonable. Another possible explanation is that other variations, which reside in the GG (558Arg-1988Arg) haplotype, such as c.6255T>C in the 3′-UTR, might change the stability of the mRNA leading to a protective effect on arrhythmias. In this regard Yang *et al.* (2004) demonstrated that –92C>A located in the promoter of *SCN5A* increased luciferase activity in neonatal cardiac myocytes. They proposed that this polymorphism might represent the first example of an allele that could protect against serious arrhythmias.

Comparison of the allele frequencies between patients and controls clearly suggests that c.703 + 130G>A is associated with an increased risk of arrhythmias, although the functional role of this SNP remains unknown. Because the haplotype AT in patients was 3 times as common as in the controls, we could not rule out the possibility that c.703+130G>A is linked with an unidentified variation that influences susceptibility to cardiac arrhythmias. In the dbSNP database of NCBI many SNPs were reported in introns 5 and 6, proximal to c.703+130G>A, including rs6797133, rs6786119, rs6776383, rs6791081 and rs6793943. Further analyses are needed to reveal a haplotype containing c.703+130G>A that increases the risk for arrhythmias.

In conclusion, 69 genetic variations, including 54 novel ones, were detected in *SCN5A*. Eleven novel missense variations were found in eleven different individuals, of which 6 were found in arrhythmic patients and 5 were in healthy controls. Another novel missense variation (p.Leu1988Arg) was found in the patients at a significantly lower frequency than in the healthy controls ($p<0.05$). Furthermore, the frequency of a novel intronic SNP, c.703+130G>A, was significantly higher in the patients than in the controls. The analysis of LD and haplotype structures of *SCN5A* revealed the possibility that the haplotype harbouring p.Leu1988Arg and p.His558Arg is associated with protection against arrhythmias. These results indicate that some genetic variations and haplotypes of *SCN5A* are positively or negatively associated with cardiac rhythm disturbance in Japanese. These findings provide fundamental information necessary to further elucidate the effects of genetic variations of *SCN5A* on channel function and cardiac rhythm.

Acknowledgments

This work was supported in part by the Program for Promotion of Fundamental Studies in Health Sciences (MPJ -3 and -6) of the Pharmaceuticals and Medical Devices Agency (PMDA).

References

Ackerman, M. J., Siu, B. L., Sturner, W. Q., Tester, D. J., Valdivia, C. R., Makielski, J. C. & Towbin, J. A. (2001) Postmortem molecular analysis of SCN5A defects in sudden infant death syndrome. *JAMA* **286**, 2264–2269.

Akai, J., Makita, N., Sakurada, H., Shirai, N., Ueda, K., Kitabatake, A., Nakazawa, K., Kimura, A. & Hiraoka, M. (2000) A novel SCN5A mutation associated with idiopathic ventricular fibrillation without typical ECG findings of Brugada syndrome. *FEBS Lett* **479**, 29–34.

Balser, J. R. (1999) Structure and function of the cardiac sodium channels. *Cardiovasc Res* **42**, 327–338.

Balser, J. R. (2001) Inherited sodium channelopathies: novel therapeutic and proarrhythmic molecular mechanisms. *Trends Cardiovasc Med* **11**, 229–237.

Bezzina, C. R., Rook, M. B. & Wilde, A. A. (2001) Cardiac sodium channel and inherited arrhythmia syndromes. *Cardiovasc Res* **49**, 257–271.

Chen, Q., Kirsch, G. E., Zhang, D., Brugada, R., Brugada, J., Brugada, P., Potenza, D., Moya, A., Borggrefe, M., Breithardt, G., Ortiz-Lopez, R., Wang, Z., Antzelevitch, C., O'Brien, R. E., Schulze-Bahr, E., Keating, M. T., Towbin, J. A. & Wang, Q. (1998) Genetic basis and molecular mechanism for idiopathic ventricular fibrillation. *Nature* **392**, 293–296.

Cormier, J. W., Rivolta, I., Tateyama, M., Yang, A. S. & Kass, R. S. (2002) Secondary structure of the human cardiac Na + channel C terminus: evidence for a role of helical

structures in modulation of channel inactivation. *J Biol Chem* **277**, 9233–9241.

Fujiki, A., Usui, M., Nagasawa, H., Mizumaki, K., Hayashi, H. & Inoue, H. (1999) ST segment elevation in the right precordial leads induced with class IC antiarrhythmic drugs: insight into the mechanism of Brugada syndrome. *J Cardiovasc Electrophysiol* **10**, 214–218.

Gellens, M. E., George, A. L., Jr., Chen, L. Q., Chahine, M., Horn, R., Barchi, R. L. & Kallen, R. G. (1992) Primary structure and functional expression of the human cardiac tetrodotoxin-insensitive voltage-dependent sodium channel. *Proc Natl Acad Sci U S A* **89**, 554–558.

Iwasa, H., Itoh, T., Nagai, R., Nakamura, Y. & Tanaka, T. (2000) Twenty single nucleotide polymorphisms (SNPs) and their allelic frequencies in four genes that are responsible for familial long QT syndrome in the Japanese population. *J Hum Genet* **45**, 182–183.

Kitamura, Y., Moriguchi, M., Kaneko, H., Morisaki, H., Morisaki, T., Toyama, K. & Kamatani, N. (2002) Determination of probability distribution of diplotype configuration (diplotype distribution) for each subject from genotypic data using the EM algorithm. *Ann Hum Genet* **66**, 183–193.

Makielski, J. C., Ye, B., Valdivia, C. R., Pagel, M. D., Pu, J., Tester, D. J. & Ackerman, M. J. (2003) A ubiquitous splice variant and a common polymorphism affect heterologous expression of recombinant human SCN5A heart sodium channels. *Circ Res* **93**, 821–828.

Makita, N., Horie, M., Nakamura, T., Ai, T., Sasaki, K., Yokoi, H., Sakurai, M., Sakuma, I., Otani, H., Sawa, H. & Kitabatake, A. (2002) Drug-induced long-QT syndrome associated with a subclinical *SCN5A* mutation. *Circulation* **106**, 1269–1274.

Mok, N. S., Priori, S. G., Napolitano, C., Chan, K. K., Bloise, R., Chan, H. W., Fung, W. H., Chan, Y. S., Chan, W. K., Lam, C., Chan, N. Y. & Tsang, H. H. (2004) Clinical profile and genetic basis of Brugada syndrome in the Chinese population. *Hong Kong Med J* **10**, 32–37.

Paulussen, A. D., Gilissen, R. A., Armstrong, M., Doevendans, P. A., Verhasselt, P., Smeets, H. J., Schulze-Bahr, E., Haverkamp, W., Breithardt, G., Cohen, N. & Aerssens, J. (2004) Genetic variations of KCNQ1, KCNH2, SCN5A, KCNE1, and KCNE2 in drug-induced long QT syndrome patients. *J Mol Med* **82**, 182–188.

Priori, S. G., Napolitano, C., Gasparini, M., Pappone, C., Della Bella, P., Giordano, U., Bloise, R., Giustetto, C., De Nardis, R., Grillo, M., Ronchetti, E., Faggiano, G. & Nastoli, J. (2002) Natural history of Brugada syndrome: insights for risk stratification and management. *Circulation* **105**, 1342–1347.

Schott, J. J., Alshinawi, C., Kyndt, F., Probst, V., Hoorntje, T. M., Hulsbeek, M., Wilde, A. A., Escande, D., Mannens, M. M. & Le Marec, H. (1999) Cardiac conduction defects associate with mutations in *SCN5A*. *Nat Genet* **23**, 20–21.

Schulze-Bahr, E., Eckardt, L., Breithardt, G., Seidl, K., Wichter, T., Wolpert, C., Borggrefe, M. & Haverkamp, W. (2003) Sodium channel gene (*SCN5A*) mutation in 44 index patients with Brugada syndrome: different incidences in familial and sporadic disease. *Hum Mutat* **21**, 651–652.

Schwartz, P. J., Priori, S. G., Locati, E. H., Napolitano, C., Cantu, F., Towbin, J. A., Keating, M. T., Hammoude, H., Brown, A. M. & Chen, L. S. (1995) Long QT syndrome patients with mutations of the *SCN5A* and HERG genes have differential responses to Na+channel blockade and to increases in heart rate. Implications for gene-specific therapy. *Circulation* **92**, 3381–3386.

Splawski, I., Timothy, K. W., Tateyama, M., Clancy, C. E., Malhotra, A., Beggs, A. H., Cappuccio, F. P., Sagnella, G. A., Kass, R. S. & Keating, M. T. (2002) Variant of *SCN5A* sodium channel implicated in risk of cardiac arrhythmia. *Science* **297**, 1333–1336.

Takahata, T., Yasui-Furukori, N., Sasaki, S., Igarashi, T., Okumura, K., Munakata, A. & Tateishi, T. (2003) Nucleotide changes in the translated region of *SCN5A* from Japanese patients with Brugada syndrome and control subjects. *Life Sci* **72**, 2391–2399.

Tan, H. L., Bezzina, C. R., Smits, J. P., Verkerk, A. O. & Wilde, A. A. (2003) Genetic control of sodium channel function. *Cardiovasc Res* **57**, 961–973.

Vatta, M., Dumaine, R., Varghese, G., Richard, T. A., Shimizu, W., Aihara, N., Nademanee, K., Brugada, R., Brugada, J., Veerakul, G., Li, H., Bowles, N. E., Brugada, P., Antzelevitch, C. & Towbin, J. A. (2002) Genetic and biophysical basis of sudden unexplained nocturnal death syndrome (SUNDS), a disease allelic to Brugada syndrome. *Hum Mol Genet* **11**, 337–345.

Viswanathan, P. C., Benson, D. W. & Balser, J. R. (2003) A common *SCN5A* polymorphism modulates the biophysical effects of an *SCN5A* mutation. *J Clin Invest* **111**, 341–346.

Wang, Q., Shen, J., Splawski, I., Atkinson, D., Li, Z., Robinson, J. L., Moss, A. J., Towbin, J. A. & Keating, M. T. (1995) *SCN5A* mutations associated with an inherited cardiac arrhythmia, long QT syndrome. *Cell* **80**, 805–811.

Wang, Q., Li, Z., Shen, J. & Keating, M. T. (1996) Genomic organization of the human *SCN5A* gene encoding the cardiac sodium channel. *Genomics* **34**, 9–16.

Yang, P., Kanki, H., Drolet, B., Yang, T., Wei, J., Viswanathan, P. C., Hohnloser, S. H., Shimizu, W., Schwartz, P. J., Stanton, M., Murray, K. T., Norris, K., George, A. L., Jr. & Roden, D. M. (2002) Allelic variants in long-QT disease genes in patients with drug-associated torsades de pointes. *Circulation* **105**, 1943–1948.

Yang, P., Kupershmidt, S. & Roden, D. M. (2004) Cloning and initial characterization of the human cardiac sodium channel (*SCN5A*) promoter. *Cardiovasc Res* **61**, 56–65.

Ye, B., Valdivia, C. R., Ackerman, M. J. & Makielski, J. C. (2003) A common human *SCN5A* polymorphism modifies expression of an arrhythmia causing mutation. *Physiol Genomics* **12**, 187–193.

Zhao, J. H., Curtis, D. & Sham, P. C. (2000) Model-free analysis and permutation tests for allelic associations. *Hum Hered* **50**, 133–139.

Received: 9 August 2004
Accepted: 5 November 2004

Supplementary Material

The following material is available from http://www.blackwellpublishing.com/products/journals/suppmat/ahg/ahg167/ahg167sm.htm

Am J Physiol Heart Circ Physiol 290: H1660–H1670, 2006.
First published November 4, 2005; doi:10.1152/ajpheart.00100.2004.

Multiple transcripts of Ca^2 channel $_1$-subunits and a novel spliced variant of the $_{1C}$-subunit in rat ductus arteriosus

Utako Yokoyama,[1,2] Susumu Minamisawa,[2,4] Satomi Adachi-Akahane,[5] Toru Akaike,[1] Isao Naguro,[6] Kengo Funakoshi,[3] Mari Iwamoto,[1] Masamichi Nakagome,[2] Nobuyuki Uemura,[2] Hideaki Hori,[2] Shumpei Yokota,[1] and Yoshihiro Ishikawa[2,7]

Departments of [1]Pediatrics, [2]Physiology, and [3]Neuroanatomy, Yokohama City University, Yokohama; [4]Consolidated Research Institute for Advanced Science and Medical Care, Waseda University; [5]Department of Pharmacology, School of Medicine, Faculty of Medicine, Toho University, Tokyo; [6]Laboratory of Cell Signaling, Graduate School of Pharmaceutical Sciences, The University of Tokyo, Tokyo, Japan; and [7]Cardiovascular Research Institute, Departments of Cell Biology and Molecular Medicine and Medicine (Cardiology), New Jersey Medical School, Newark, New Jersey

Submitted 3 February 2004; accepted in final form 27 October 2005

Yokoyama, Utako, Susumu Minamisawa, Satomi Adachi-Akahane, Toru Akaike, Isao Naguro, Kengo Funakoshi, Mari Iwamoto, Masamichi Nakagome, Nobuyuki Uemura, Hideaki Hori, Shumpei Yokota, and Yoshihiro Ishikawa. Multiple transcripts of Ca^2 channel $_1$-subunits and a novel spliced variant of the $_{1C}$-subunit in rat ductus arteriosus. *Am J Physiol Heart Circ Physiol* 290: H1660–H1670, 2006. First published November 4, 2005; doi:10.1152/ajpheart.00100.2004.—Voltage-dependent Ca^2 channels (VDCCs), which consist of multiple subtypes, regulate vascular tone in developing arterial smooth muscle, including the ductus arteriosus (DA). First, we examined the expression of VDCC subunits in the Wistar rat DA during development. Among $_1$-subunits, $_{1C}$ and $_{1G}$ were the most predominant isoforms. Maternal administration of vitamin A significantly increased $_{1C}$- and $_{1G}$-transcripts. Second, we examined the effect of VDCC subunits on proliferation of DA smooth muscle cells. We found that 1 M nitrendipine (an L-type Ca^2 channel blocker) and kurtoxin (a T-type Ca^2 channel blocker) significantly decreased [^{3}H]thymidine incorporation and that 3 M efonidipine (an L- and T-type Ca^2 channel blocker) further decreased [^{3}H]thymidine incorporation, suggesting that L- and T-type Ca^2 channels are involved in smooth muscle cell proliferation in the DA. Third, we found that a novel alternatively spliced variant of the $_{1C}$-isoform was highly expressed in the neointimal cushion of the DA, where proliferating and migrating smooth muscle cells are abundant. The basic channel properties of the spliced variant did not differ from those of the conventional $_{1C}$-subunit. We conclude that multiple VDCC subunits were identified in the DA, and, in particular, $_{1C}$- and $_{1G}$-subunits were predominant in the DA. A novel spliced variant of the $_{1C}$-subunit gene may play a distinct role in neointimal cushion formation in the DA.

alternative spliced; development; gene expression; fetal circulation

THE DUCTUS ARTERIOSUS (DA) is a fetal arterial connection between the pulmonary artery and the descending aorta. After birth, the DA closes immediately, in accordance with its smooth muscle contraction. An increase in oxygen tension and a dramatic decline in circulating prostaglandins are the most important triggers of DA contraction (5). Generally, vascular smooth muscle contraction is induced by Ca^2 / calmodulin-dependent phosphorylation of the regulatory myosin light chain, which is mediated by an increase in intracellular Ca^2 . Ca^2 influx through voltage-dependent Ca^2 channels (VDCCs) and Ca^2 release from intracellular stores are major sources of this increase (8, 26). Thus VDCCs must play an important role in vascular myogenic reactivity and tone of the DA.

VDCCs are classified, according to their distinct electrophysiological and pharmacological properties, into low (T-type) and high (L-, N-, P-, Q-, and R-type) VDCCs (20, 39). VDCCs consist of different combinations of $_1$-subunits and auxiliary subunits. The $_1$-subunit forms the ion-conducting pore, the voltage sensor, and the interaction sites for Ca^2 channel blockers and activators (15). Therefore, $_1$-subunits principally determine the channel character of VDCCs. Ten $_1$-subunit isoforms have been identified. Four $_2$ -subunit complexes and four -subunits, which modulate the trafficking and the biophysical channel properties of $_1$-subunits (1), have been identified (3). Although some studies have investigated the role of VDCCs in the DA (28, 37), characterization of VDCCs, including the composition of each subunit, the developmental change in their expression, and their physiological roles, remains poorly understood.

In addition to their role in determining contractile state, a growing body of evidence has demonstrated that VDCCs play an important role in regulating differentiation and remodeling of vascular smooth muscle cells (SMCs) (14, 17, 41). The DA dramatically changes its morphology during development. Intimal cushion formation during development is a characteristic feature of vascular remodeling of the DA (10, 30). Intimal cushion formation involves many cellular processes, including an increase in SMC migration and proliferation, production of hyaluronic acid under the endothelial layer, and impairment of elastin fiber assembly. The role of VDCCs in vascular remodeling of the DA has not been investigated.

In the present study, we identified multiple VDCC subunits in the DA by semiquantitative and quantitative RT-PCR and immunodetection. In particular, $_{1C}$- and $_{1G}$-subunits were predominant in the DA. Furthermore, we will demonstrate the identification of a novel spliced variant of the $_{1C}$-subunit gene that may play a role in neointimal cushion formation of the DA.

Address for reprint requests and other correspondence: S. Minamisawa, Dept. of Physiology, Yokohama City Univ., 3-9 Fukuura, Kanazawa-ku, Yokohama 236-0004, Japan (e-mail: sminamis@med.yokohama-cu.ac.jp).

The costs of publication of this article were defrayed in part by the payment of page charges. The article must therefore be hereby marked "*advertisement*" in accordance with 18 U.S.C. Section 1734 solely to indicate this fact.

Table 1. *Oligonucleotides used for RT-PCR*

Gene	Accession No.	Forward (5 -3)	Position	Reverse (5 -3)	Position	Size, bp	Annealing Temperature, °C
$Ca_v1.1$ (1S)	U31816	cgcgaggtcatggacgtggag	572–592	gatcaccagccagtagaagac	695–715	144	60
$Ca_v1.2$ (1C)-1	AF394939	ggagagttttccaaagagagg	1342–1362	gatcaccagccagtagaagac	1699–1719	378	60
$Ca_v1.2$ (1C)-2	AF394939	tggaaactcagctctaagag	5551–5570	tcctggtaggagagtatatc	5695–5714	164	54
$Ca_v1.3$ (1D)	NM_017298	attctgaacatggtcttcacg	4246–4265	gattctattgctctcttcaga	4405–4425	180	55
$Ca_v1.4$ (1F)	NM_053701	gcagatggcccttcaatctc	001–020	ccatgtcggatcccaggaag	833–852	852	57
$Ca_v3.1$ (1G)	NM_031601	aatggcaagtcggcttca	3648–3665	caggagacgaaaccttga	3837–3854	207	50
$Ca_v3.2$ (1H)	AF290213	gacgaggataagacgtct	3111–3128	ggagacgcgtagcctgtt	3906–3923	813	57
$Ca_v3.3$ (1I)	NM_020084	gatgaggaccagagctca	2768–2785	tctggctgcagtgagaggc	2943–2961	194	60
2 1	NM_012919	tggtgtgatgggcgttgatgtgtc	1741–1764	gtcattgc-agtattcccttggtgc	2234–2258	518	56
2 2	NM_175592	aggttcttcagtgaggtggat	2749–2769	ttataggacgcgttcaccgag	3081–3101	353	62
2 3	NM_175595	ggcacagatgtcccagtaaaaga	1483–1505	tgtgtagtagtagtcattggtcat	1780–1803	321	58
1-1	NM_017346	tgacaactccagttccag	624–641	tcaagaagtcaaacaacg	835–852	229	62
1-2	NM_017346	tcaatgtccaaatagcag	1163–1180	tgtcagcatcaaaggtgtc	1555–1573	411	56
2	NM_053851	acagagagcaaagcaagggaat	771–792	tctccttgagaaccctgtgaatt	1693–1715	945	56
3	NM_012828	gtggtgttggatgctgac	892–909	attgtggtcatgctccga	1483–1500	609	58
4	XM_215742	cgattcggcaagagagagaacagcaag	396–422	gtttgggcagcctcaaagcctatgtcg	1730–1756	1361	58
GAPDH	AF106860	cccatcaccatcttccaggagcg	1060–1082	gcagggatgatgttctgggctgcc	1446–1469	410	55

MATERIALS AND METHODS

Animals. All animals were cared for in compliance with the guiding principles of the American Physiological Society. The experiments were approved by the Ethical Committee of Animal Experiments of Yokohama City University School of Medicine.

Maternal vitamin A administration. Maturation of the fetal DA was accelerated by maternal administration of vitamin A, as described previously (25, 42). Briefly, vitamin A [retinyl palmitate, 33 mg, which is equivalent to 18 mg of retinol (Eisai, Tokyo, Japan)] was diluted in polyoxyethylene castor oil and injected intramuscularly into pregnant Wistar rats daily from *day 17* of gestation in a dose of 1 mg (3,000 IU)/kg body wt.

Tissue collection and preparation. For developmental studies, we used pooled tissues obtained from Wistar rat embryos on embryonic *days 19* (e19, *n* 60) and *21* (e21, *n* 90) and from neonates on the day of birth (*day 0*, *n* 60). After excision, tissues were immediately frozen in liquid nitrogen and stored at 80°C.

Semiquantitative and quantitative RT-PCR. Total RNA was isolated from the tissues using TRIzol, as recommended by the manufacturer (Invitrogen, La Jolla, CA). Genomic DNA was digested by DNase I before RT reaction. After annealing to random hexamer, 2 M total RNA was reverse transcribed to cDNA by SuperScript II RT (Invitrogen). For semiquantitative RT-PCR analyses of VDCC subunits, the primers for PCR amplification were designed on the basis of the rat nucleotide sequences of VDCCs (Table 1) to amplify cDNA between two exons, except 1S-subunit primers. The PCR cycle consisted of denaturation at 94°C for 30 s, annealing at each temperature for 30 s, and elongation at 72°C for 30 s; 35–40 forty cycles were performed. Amplification products were analyzed by 2% agarose gel electrophoresis and ethidium bromide staining. A fragment of GAPDH was amplified as internal control. For quantitative RT-PCR analysis, sequences for PCR primers are listed in Table 2. The spliced variant of the 1C-subunit and nonspliced isoform were detected simultaneously by $Ca_v1.2$ (1C)-4 primer. Amplification and detection were performed as described previously (40). Each template was tested at least three times to confirm the reproducibility of the assays. The abundance of each gene was determined relative to GAPDH using TaqMan rodent GAPDH control reagents kits (Applied Biosystems, Foster City, CA). For each RT-PCR experiment, we included RT negative control and confirmed no amplification in each reaction.

Restriction enzyme analysis. The relative abundance of high-voltage-activated (HVA) channels of the 1-subunits was determined in the DA as described previously (29). Briefly, all HVA channels of the 1-subunits were amplified by RT-PCR using the following set of primers: at(c/t) (a/g)tc acc ttc cag gag ca (forward) and gcg tag atg aag aa(a/g/c) agc at (reverse). Five restriction enzymes selectively cut the 1A-, 1B-, 1C-, 1D-, and 1E-isoforms of the PCR products. The intensity of the digested fragments in correspondence to each isoform was measured by a FujiFilm image analysis system (Image Gauge version 3.41).

Generation of polyclonal antibody against spliced variant of 1C-subunit. We generated a polyclonal antibody against spliced variant of rat 1C-subunit using a keyhole limpet hemocyanin-conjugated synthetic peptide for immunization. Antigens for spliced variant of anti-rat 1C-subunit antibody were derived from the I-II cytoplasmic loop region spanning amino acids 59–71 of the spliced variant of rat

Table 2. *Oligonucleotides used for quantitative RT-PCR*

Gene	Accession No.	Forward (5 -3)	Position	Reverse (5 -3)	Position	Probe (5 -3)	Position	Size, bp
$Ca_v1.2$ (1C)-3	AF394939	tgattgttgtgg-gtagcattgtt	3992–4014	tcatagagggaga-gcattgggtat	4049–4072	tagcaatcaccgaggtacacc-cagctg (FAM)	4019–4072	81
$Ca_v1.2$ (1C)-4	AY323810	aatgaggacgag-ggcatgg	136–154	gcccacaagtgag-actgagtctg	258–280	agggaaatttgcttggtttag-tcactccaca (FAM)	210–241	145
	AF394939					tgaagacaaaccccgaaacat-gagca (VIC)	1497–1522	70
$Ca_v1.3$ (1D)	NM_017298	gaagaggacgag-cctgaggtt	3028–3048	ttttctccttcat-gttcaactctga	3076–3100	(SYBR)		73
$Ca_v3.1$ (1G)	NM_031601	cctgatttcttt-tcgcccag	3054–3073	tggcaaaaggc-tctttcgtag	3138–3158	(SYBR)		105

$_{1C}$-subunit (RGAPAGLHDQKKG C). A male Japanese White rabbit was immunized four times every 2 wk. Serum was collected, and polyclonal antibody was affinity purified.

Immunoblotting. The membrane fraction was prepared and immunoblotting was performed as described previously (23). Briefly, tissues from rat (DA, aorta, atria, left ventricle, and lung) were homogenized in an ice-cold buffer [in mM: 50 Tris (pH 8.0), 1 EDTA, 1 EGTA, 1 dithiothreitol, and 200 sucrose] and protease inhibitors (Complete Mini, Roche, Tokyo, Japan). The polyclonal antibody specific for $_{1C}$-, $_{1D}$-, and $_{1G}$-subunits (Chemicon, Temecula, CA) or spliced variant of $_{1C}$-subunit at 5 g/ml was used to examine 20- g membrane fractions from rat tissues.

Immunohistochemistry. For immunoperoxidase demonstration of VDCCs in the DA, paraffin-embedded blocks containing DA tissues were cut into 4- m-thick sections and placed on 3-aminopropyltriethoxysilane-coated glass slides. To determine the boundary line of intimal cushion formation, tissue sections were stained with Elastica van Gieson as recommended by the manufacturer (Muto Pure Chemicals). The specimens were deparaffinized, rehydrated, and incubated for 5 min in peroxidase-blocking reagent (DAKO Laboratories) to inactivate endogenous peroxidases. Slides were incubated with each primary antibody of splicing variant of $_{1C}$-, $_{1D}$-, $_{1G}$-, and $_{1C}$-subunits (1:200 dilution) at room temperature for 30 min. After they were washed with 0.1 M PBS for 5 min, the slides were incubated for 30 min in biotinylated rabbit anti-goat IgG (Vector, Burlingame, CA). Then the slides were washed with 0.1 M PBS for 5 min, incubated for 30 min in avidin-biotin-horseradish peroxidase complex (Vector), and washed again with 0.1 M PBS for 5 min. The peroxidase reactivity was demonstrated with 3,3'-diaminobenzidine (Sigma, St. Louis, MO) and 0.3% H_2O_2 for 5 min. The specificity of staining was examined by omission of the primary antibodies. The slides were counterstained with Mayer's hematoxylin.

Primary culture of rat DA SMCs. Vascular SMCs in primary culture were obtained from the DA of Wistar rat embryos at e21. The tissues were minced and transferred to a 1.5-ml centrifuge tube that contained 800 l of collagenase-dispase enzyme mixture [1.5 mg/ml collagenase-dispase (Roche), 0.5 mg/ml elastase type II-A (Sigma Immunochemicals, St. Louis, MO), 1 mg/ml trypsin inhibitor type I-S (Sigma), and 2 mg/ml bovine serum albumin fraction V (Sigma) in Hanks' balanced salt solution (Sigma)]. The digestion was carried out at 37°C for 15–20 min. Then cell suspensions were centrifuged, and the medium was changed to the collagenase II enzyme mixture [1 mg/ml collagenase II (Worthington), 0.3 mg/ml trypsin inhibitor type I-S, and 2 mg/ml bovine serum albumin fraction V in Hanks' balanced salt solution]. After 12 min of incubation at 37°C, cell suspensions were transferred to growth medium in 35-mm poly-L-lysine (Sigma)-

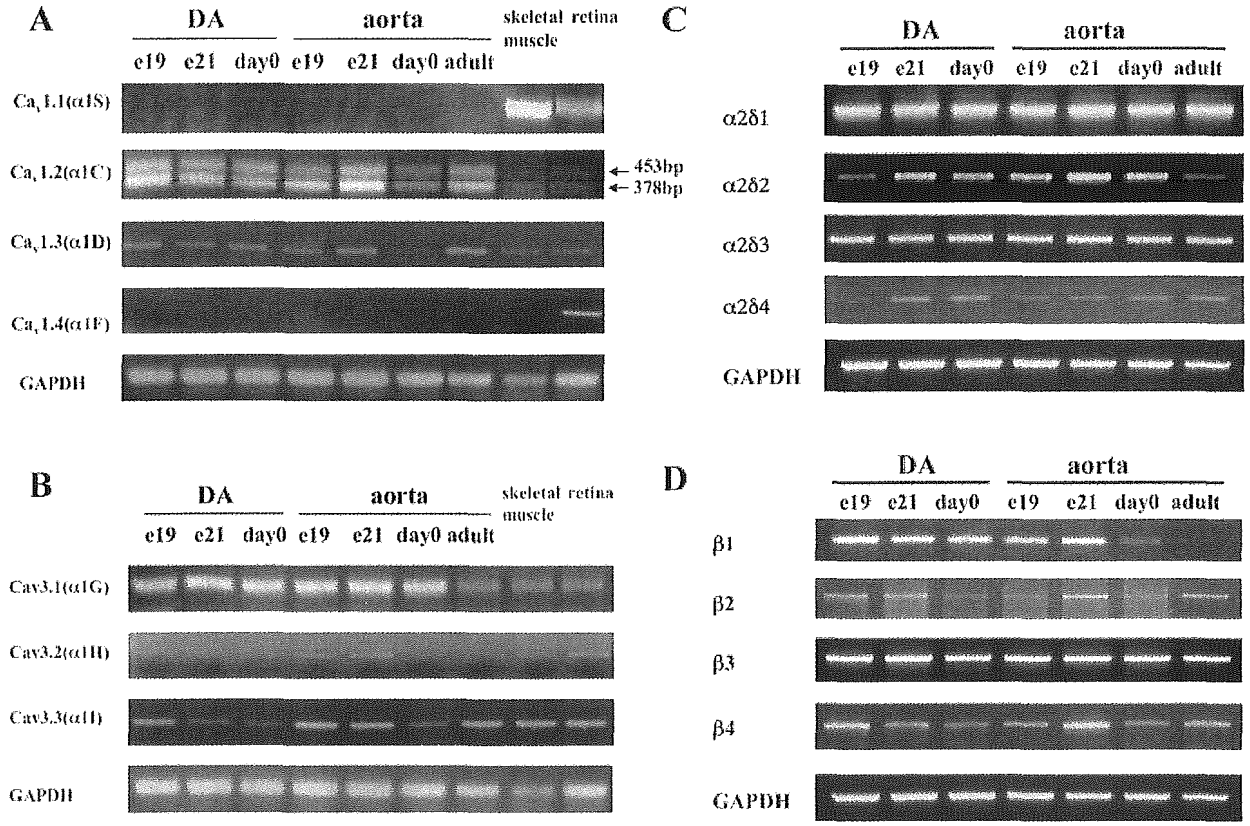

Fig. 1. Semiquantitative RT-PCR analyses of Ca^2 channel subunits. *A*: RT-PCR for L-type Ca^2 channel $_1$-subunit isoforms in rat ductus arteriosus (DA), aorta, skeletal muscle, and retina. RNA samples from tissues were processed for 35 cycles of PCR using primers directed to the cDNA sequence of VDCC $_{1S}$-, $_{1C}$-, $_{1D}$-, and $_{1F}$-isoforms. PCR of the primer alone, without template, resulted in no product (data not shown). Transcripts for $_{1C}$- and $_{1D}$-subunits were detected in DA and aorta, but no transcripts for $_{1S}$- and $_{1F}$-subunits were detected in DA and aorta. Transcripts for $_{1C}$-subunit were detected as clear bands of expected (378 bp) and longer (453 bp) lengths. Sequence analysis detected insertion of an unreported 75-bp cDNA in the 453-bp band into the 378-bp band. Expression of $_{1C}$-subunit mRNA was not altered during development. Expression of $_{1D}$-subunit mRNA was decreased in DA from embryonic *day 21* (e21) but decreased from *day 0* (birth) in aorta. *B*: RT-PCR for T-type Ca^2 channel $_{1G}$-, $_{1H}$-, and $_{1I}$-subunits in rat DA, aorta, skeletal muscle, and retina. Transcripts for these subunits were present in DA and aorta. Expression level of $_{1G}$-subunit mRNA was high from embryonic *day 19* (e19) to *day 0* in DA and aorta and decreased in adult aorta. Levels of $_{1H}$- and $_{1I}$-subunit mRNA expression were low in DA and aorta. *C*: RT-PCR for $_2$ -subunits in rat DA and aorta during development. Transcripts for all 4 $_2$ -subunit isoforms were present in both tissues. *D*: RT-PCR for -subunits in rat DA and aorta during development. Transcripts for 4 -isoforms were present in both tissues. $_3$-Subunit mRNA was abundant in DA and aorta throughout development.

coated dishes in a moist tissue culture incubator at 37°C in 5% CO_2-95% ambient mixed air. The growth medium contained DMEM with 10% FCS, 100 U/ml penicillin, and 100 mg/ml streptomycin (Invitrogen). The confluent cells were used at *passages 4–6*. We confirmed that 99% of cells were positive for -smooth muscle actin and showed the typical "hill-and-valley" morphology.

Cell proliferation assays. [^{3}H]thymidine incorporation was used to measure cell proliferation in DA SMCs. The SMCs were reseeded into a 24-well culture plate at an initial density of 1 10^5 cells per well for 24 h before serum starvation with DMEM containing 0.5% FCS. Cells were then incubated with or without nitrendipine (1 M), kurtoxin (1 M), and efonidipine (3 M) for 16 h in the starvation medium before addition of 1 Ci of [*methyl*-^{3}H]thymidine (specific activity 5 Ci/mM; Amersham International, Bucks, UK) for 4 h at 37°C. After fixation with 1.0 ml of 10% trichloroacetic acid, the cells were solubilized with 0.5 ml of 0.5 M NaOH and then neutralized with 0.25 ml of 1 N HCl. A liquid scintillation counter was used to measure [^{3}H]thymidine incorporation. Data obtained from triplicate wells were averaged.

Generation of expression construct for spliced variant of rat $_{1C}$-subunit. The 220-bp fragment containing a 75-bp insertion of the spliced variant of rat VDCC $_{1C}$-subunit was extracted from the 453-bp PCR fragment using *Xho* I and *Sph* I restriction enzymes. Then the 220-bp fragment was introduced into the *Xho* I/*Sph* I site of the pcDNA3.1( )-based expression construct of the rat brain 1C subunit (rbCII; kindly supplied by Dr. T. P. Snutch) (35). The sequence of the expression construct was confirmed by direct sequencing analysis.

Electrophysiological recordings. $Ca_V1.2$ (rbCII; GenBank accession no. M67515) or its mutant was transiently expressed in BHK6 cells, which stably express $_1$- and $_2$ -subunits. Transfection was carried out with a transfection reagent (FuGene 6, Roche), as previously described (43).

Electrophysiological recordings were performed in the whole cell patch-clamp configuration using a patch/whole cell-clamp amplifier (Axopatch 200B, Axon Instruments) and an analog-to-digital converter (Digidata 1200, Axon Instruments) (43). Data acquisition was performed with pCLAMP7 software (Axon Instruments). Signals were filtered at 5 kHz. Capacitative currents were electrically compensated. The P/4 protocol (pCLAMP7) was used for leak subtraction. Ca^2 currents and Ba^2 currents (I_{Ba}) through $Ca_V1.2$ (rbCII) Ca^2 channels expressed in BHK6 cells were measured as previously described (27). The external solution contained (in mM) 137 NaCl, 5.4 KCl, 1 $MgCl_2$, 10 HEPES, and 10 glucose, with 2 $CaCl_2$ or $BaCl_2$ as a charge carrier; pH was adjusted to 7.4 with NaOH at room temperature. The resistance of the patch electrode was 2–2.5 M when it was filled with the pipette solution containing (in mM) 120 $CsMeSO_4$, 20 TEA-Cl, 14 EGTA, 5 Mg-ATP, 5 Na_2 creatine phosphate, 0.2 GTP, and 10 HEPES, with pH adjusted to 7.3 with CsOH at room temperature. All experiments were carried out at room temperature.

The half-activation potential ($V_{h\text{-}act}$) was estimated by fitting the current-voltage (*I-V*) relations (curves) to the following equation by an interactive nonlinear regression fitting procedure

$$I \quad V_m \quad V_{rev} \quad G_{max} \quad 1/1 \quad \exp V_m \quad V_{h\text{-}act} /k$$

where V_m is membrane potential, V_{rev} is reversal potential, k is slope factor, and G_{max} is maximum conductance.

Half-inactivation voltage ($V_{h\text{-}inact}$) was estimated by fitting the steady-state inactivation curves to the following equation

$$I \quad I_{min} \quad I_{max} \quad I_{min} / 1 \quad \exp V_{h\text{-}inact} \quad V /k$$

where I_{max} and I_{min} are maximum and minimum plateau currents, respectively, and k is slope factor.

Statistical analysis. Values are means SE. Student's unpaired *t*-tests and unpaired ANOVA followed by the Student-Newman-Keuls test were used for statistical analysis. P 0.05 was considered statistically significant.

RESULTS

Multiple transcripts of VDCC $_1$-, $_2$ -, and -subunits in rat DA. Semiquantitative RT-PCR analyses revealed that, among voltage-dependent L-type Ca^2 channel subunits, $_{1C}$- and $_{1D}$-subunit mRNAs were expressed in the DA and the aorta, whereas neither $_{1F}$- nor $_{1S}$-subunit transcript was detected (Fig. 1*A*). The $_{1C}$-subunit transcripts were amplified as two bands, 378 bp (the expected size) and 453 bp, in the RT-PCR products. The 378-bp band was confirmed as the reported VDCC $_{1C}$-subunit, and the 453-bp band was identified as a novel spliced variant of the rat VDCC $_{1C}$-subunit by sequencing analysis. Another spliced variant of $_{1C}$-subunit in the human, which displayed oxygen-sensitive opening of the channel, was recently identified (11). However, we could not detect this spliced variant in DA, aorta, and genomic DNA in the rat by RT-PCR using $Ca_V1.2$ ($_{1C}$)-2 primers, although we could detect its expression in human right ventricle (data not shown). The expression of VDCC $_{1A}$ (P/Q-type)-, $_{1B}$ (N-type)-, and $_{1E}$ (R-type)-subunits was not detected in the DA by semiquantitative RT-PCR (data not shown).

The transcripts of all T-type Ca^2 channel $_1$-subunits, $_{1G}$, $_{1H}$, and $_{1I}$, were detected in the DA and aorta (Fig. 1*B*). In our PCR conditions, expression of the $_{1G}$-isoform was highest and expression of the $_{1H}$-isoform was lowest in the DA among T-type Ca^2 channel $_1$-subunits. Expression of $_{1I}$ was decreased from e21 in the DA and from *day 0* in the aorta.

The transcripts of all four $_2$ -subunits were detected in the DA and aorta (Fig. 1*C*). Transcripts of all four -subunits were detected in the DA and aorta (Fig. 1*D*). Among them, $_3$-subunit mRNA was highly expressed by semiquantitative RT-PCR during development in the DA and aorta. Expression of $_3$-subunit mRNA was not changed during development. Expression of $_1$-subunit mRNA was not detected in adult aorta.

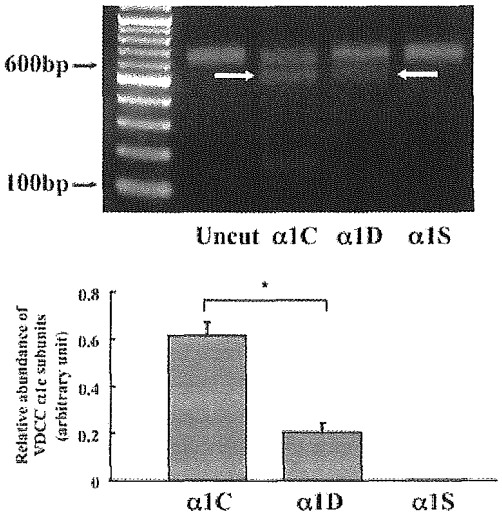

Fig. 2. Relative abundance of L-type Ca^2 channel $_1$-subunits in DA at e21. Uncut lane shows a single band corresponding to fragments obtained after RT-PCR; $_{1C}$, $_{1D}$, and $_{1S}$ lanes show fragments obtained after restriction digest with enzymes. Digested fragments are indicated by arrows. Digested fragment was detected more in $_{1C}$- than in $_{1D}$-subunit. No digested fragment was detected in $_{1S}$-subunit. Values for $_{1C}$- and $_{1D}$-subunits were obtained from the value into which elements digested by each enzyme were divided by amount of uncut PCR product using densitometry. The $_{1C}$-subunit is the most abundant of the L-type Ca^2 channel subunits. *P 0.01.

Expression $_2$- and $_4$-subunit mRNA was higher in the fetus than that in neonates on *day 0*.

VDCC $_{1C}$-subunit was a predominant transcript of L-type Ca^2 channel subunits in rat DA. Using restriction enzyme analysis as previously reported (29), we determined relative abundance of HVA Ca^2 channel mRNA. The digested fragments were detected only in the $_{1C}$- and $_{1D}$-subunit lanes (Fig. 2), which is consistent with the result from semiquantitative RT-PCR. The values of $_{1C}$- and $_{1D}$-subunits were obtained when the value into which elements digested by each enzyme was divided by the amount of uncut PCR product. The density of the digested fragment was significantly higher in the $_{1C}$- than in the $_{1D}$-subunit lane, indicating that the $_{1C}$-subunit is the most abundant transcript among L-type Ca^2 channel subunits.

Protein expression of $_{1C}$-, $_{1D}$-, $_{1G}$-, and $_3$-subunits in the DA. Protein expression of $_{1C}$-, $_{1D}$-, $_{1G}$-, and $_3$-subunits was examined by immunoblotting analysis (Fig. 3). Although the expression level of $_{1C}$-subunit mRNA was higher in the DA than in the fetal aorta, the expression level of $_{1C}$-subunit protein in the DA was comparable with that in the aorta at e21 and much less than that in the adult atrium and aorta. Protein expression of the $_{1D}$-subunit was similarly detected in the DA and aorta at e21, but not in the adult aorta. The level of $_{1G}$-subunit protein expression was high in the DA and aorta at e21 and undetectable in the adult aorta. We also detected $_3$-subunit protein expression in the DA at e21.

In addition, we examined the localization of $_{1C}$-, $_{1D}$-, and $_{1G}$-subunit proteins in the DA at e21 by immunostaining with anti- $_{1C}$, - $_{1D}$, and - $_{1G}$ (Fig. 3*B*). Strong immunoreaction of $_{1C}$- and $_{1G}$-subunits and moderate immunoreaction of the $_{1D}$-subunit were found in SMCs in the DA. Especially, the $_{1G}$-subunit was strongly expressed in the region of intimal thickening of the DA, which is clearly distinguished by Elastica stain.

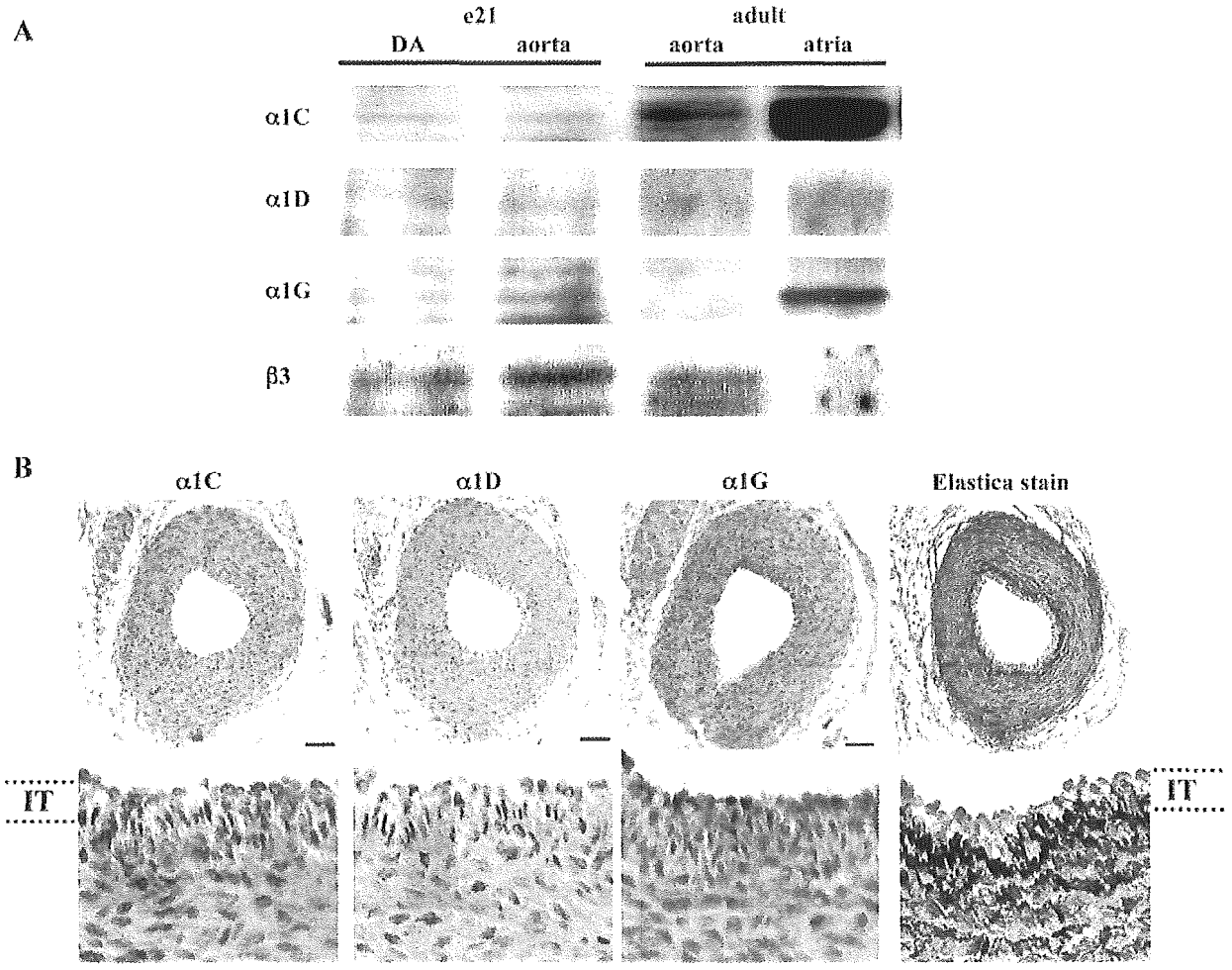

Fig. 3. *A*: expression of $_{1C}$-, $_{1D}$-, $_{1G}$-, and $_3$-subunit protein in rat DA, aorta, and atrium by immunoblotting. Membrane proteins from rat tissues were separated by SDS-PAGE, together with prestained molecular weight markers, and subjected to immunoblot analysis with each subunit-selective antibody. Expression level of $_{1C}$-subunit protein was comparable in DA and aorta at e21 and much less in DA than in adult atrium. Expression of $_{1D}$-subunit was similarly detected in DA and aorta at e21. Expression of $_{1G}$-subunit protein was high in DA and aorta at e21 and undetectable in adult aorta. Expression of $_3$-subunit was high in DA at e21. *B*: DA at e21 immunostained with anti- $_{1C}$, - $_{1D}$, and - $_{1G}$. Elastica stain identified the boundary of intimal cushion formation. High-magnification (4) image of the region of intimal cushion formation is shown at *bottom*. Strong immunoreaction of $_{1C}$-subunit and mild immunoreaction of $_{1D}$-subunit were ubiquitously found in DA. Strong $_{1G}$-subunit immunoreaction was especially found at the region of intimal thickening (IT) in DA. Scale bar, 100 m.

Effects of development and maternally administered vitamin A on expression of VDCC -subunit transcripts. Although the expression levels of -subunit mRNA were not changed in the DA during development, a significant decrease in the expression level of -subunit mRNA in the aorta resulted in a higher expression of -subunit mRNA in the DA than in the aorta after e21 (Fig. 4*A*). Maternally administered vitamin A significantly increased the expression levels of -subunit mRNA at *day 0* (*P* 0.01; Fig. 4*B*).

Expression of -subunit mRNA was 25–120 times higher in perinatal vessels than in the adult aorta (Fig. 4*C*). The expression was upregulated in the DA during development. The level of -subunit mRNA was significantly higher in the DA than in the aorta at *day 0*. Maternally administered vitamin A significantly upregulated the expression of -subunit mRNA at all developmental stages (*P* 0.001; Fig. 4*D*).

Effects of L- and T-type VDCCs on SMC proliferation in DA. We used a specific L-type VDCC blocker (nitrendipine), a specific T-type VDCC blocker (kurtoxin), and an L- and T-type VDCC blocker (efonidipine) to investigate a role for VDCCs in SMC proliferation in the DA. Significant inhibition of [^{3}H]thymidine incorporation was observed in rat DA SMCs treated with 1 M nitrendipine, 3 M efonidipine, or 1 M kurtoxin compared with untreated SMCs (Fig. 5). The inhibition was the strongest in SMCs treated with 3 M efonidipine, suggesting that the additive inhibitory effect of efonidipine on cell proliferation is due to the blockade of L- and T-type VDCCs in rat DA SMCs.

A novel spliced variant of the -subunit was highly expressed in adult lung and fetal arteries. As demonstrated above, using RT-PCR with $Ca_v1.2$ ( )-1 primers, we found a novel alternatively spliced isoform of the -subunit in the DA and aorta (Table 1). The PCR products were subcloned into a pCRII vector (Invitrogen) and sequenced. We reported the nucleotide sequence in the EMBL/GenBank nucleotide sequence databases (accession no. AY323810; Fig. 6*A*). The spliced variant contained a 26-amino acid insertion into the I-II cytoplasmic linker that interacts with the -subunit of (Fig. 6*B*). During the course of the present study, homologs of this variant have been reported in other species. Figure 6*C* shows

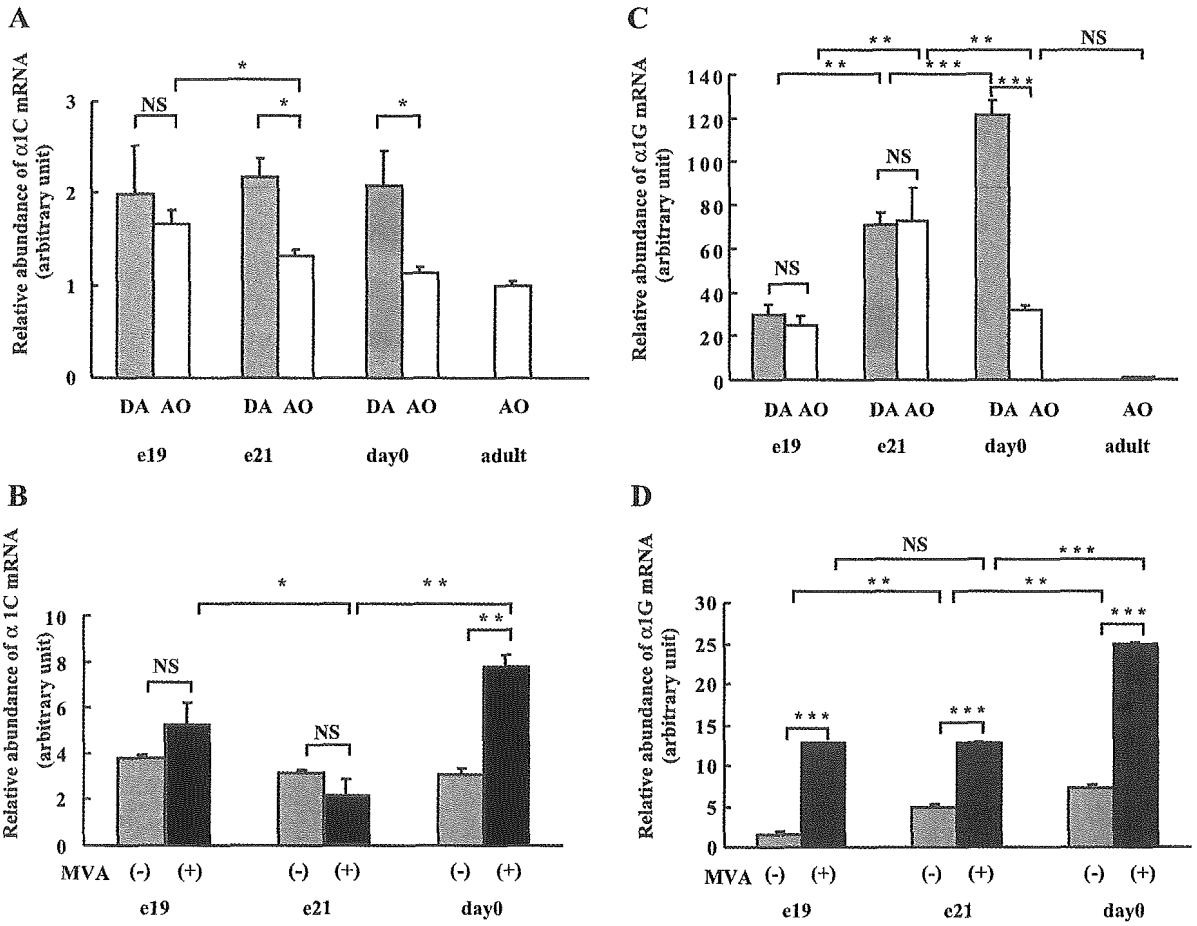

Fig. 4. *A*: developmental changes in expression of -subunit mRNA. Expression level of -subunit mRNA was higher in DA than in aorta (AO) at e21 and *day 0*. Expression level was not changed in DA during development but was decreased in aorta from e19 to e21. **P* 0.05. NS, not significant. *B*: effects of maternally administered vitamin A (MVA) on expression of -subunit mRNA in DA. Levels of -subunit mRNA were not changed in DA during development and were significantly increased with vitamin A only at *day 0*. **P* 0.05; ***P* 0.01. *C*: developmental changes in expression of -subunit mRNA. Transcripts for -subunit were increased during development in DA. Abundance of -subunit mRNA was significantly greater in DA than in aorta at *day 0*. ***P* 0.01; ****P* 0.001. *D*: effects of maternally administered vitamin A on expression of -subunit mRNA in DA. Expression of -subunit mRNA was upregulated during development and significantly higher than with vitamin A at any developmental stage. ***P* 0.01; ****P* 0.001.

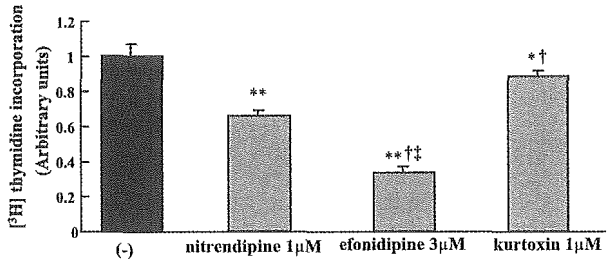

Fig. 5. Effects of VDCC blockers on [3H]thymidine uptake of DA smooth muscle cells. [3H]thymidine incorporation in groups treated with nitrendipine, efonidipine, and kurtoxin was decreased compared with that in control group in 0.1% FCS-containing medium. Treatment of DA smooth muscle cells with efonidipine resulted in additional reduction of [3H]thymidine uptake compared with nitrendipine or kurtoxin treatment. Experiments were performed 3 times independently in duplicate. Significantly different from control: *P 0.01. **P 0.0001. †Significantly different from nitrendipine (P 0.01). ‡Significantly different from kurtoxin (P 0.01).

that amino acid sequence homology between the rat and other species (mouse, rabbit, and human) is very high (100%, 92%, and 88%, respectively).

We characterized the novel spliced isoform of rat 1C-subunit. Figure 7*A* shows the expression the spliced variant of 1C-subunit mRNA and protein by semiquantitative RT-PCR and immunoblotting analyses. The PCR product migrating 453 bp was the spliced variant of the 1C-subunit and the 378-bp band indicated the reported 1C-subunit. A relatively high intensity of the 453-bp band was detected in the DA and the aorta. Using the specific antibody against the spliced variant of the 1C-subunit, we also found a high level of expression of the variant protein in arteries, including the DA, and less expression in the adult heart.

By quantitative RT-PCR analyses, the spliced variant transcript was expressed most abundantly in the adult lung (data not shown), less in the fetal arteries, and least in the adult arteries. In other adult tissues, the expression level of 1C-subunit mRNA, including this spliced variant, was very low (data not shown). The ratio of the abundance of the spliced variant to the conventional 1C-isoform was measured by quantitative RT-PCR (see MATERIALS AND METHODS). The proportion of the spliced variant and nonspliced 1C-isoform was almost invariable (1–1.5) among the lung, DA, and aorta. Furthermore, we examined the developmental changes in the expression of the spliced variant of the 1C-subunit transcript in the DA and aorta (Fig. 7*B*). The level of the spliced variant 1C-subunit mRNA peaked at e21 in the DA. After birth, the level of the spliced variant 1C-subunit mRNA was higher in the DA than in the aorta.

Localization of the spliced variant of the 1C-subunit in the DA at e21 was examined by immunostaining with anti- 1C-subunit splicing variant (Fig. 7*C*). Strong immunoreaction was found in the region of intimal thickening of the DA (Fig. 7*C*, *right*), whereas immunoreaction of the conventional 1C-isoform was ubiquitously expressed in the whole layers of the DA (Fig. 3*B*).

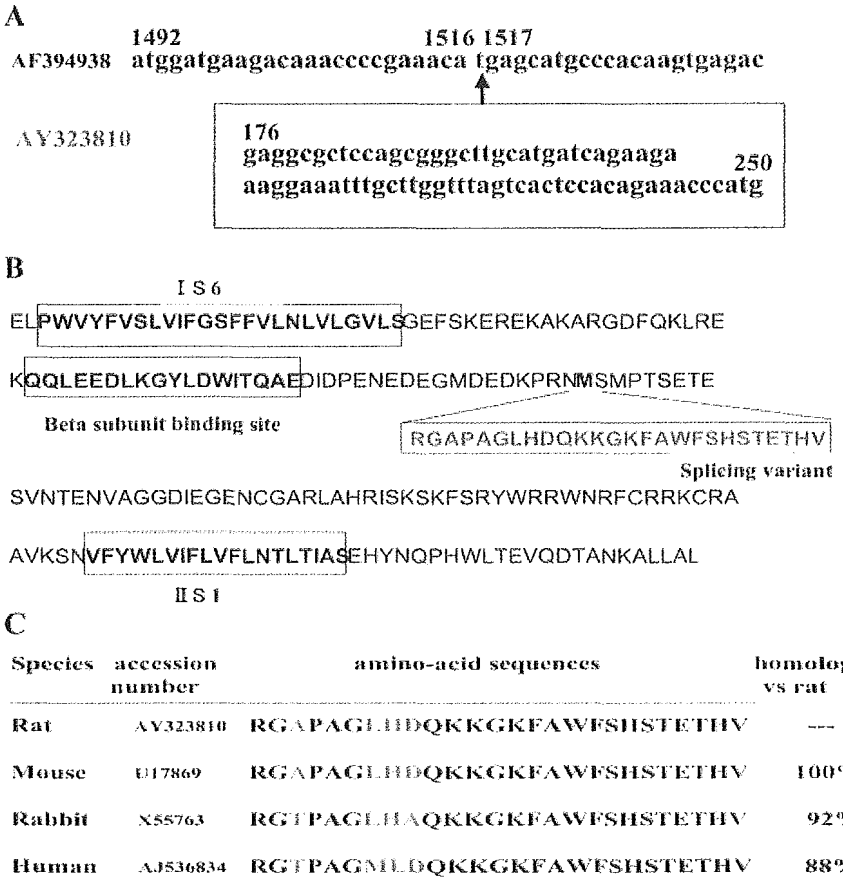

Fig. 6. *A*: alignment of nucleotide sequence of rat Ca^2 channel 1C-subunit (GenBank accession no. AF394938) and novel spliced variant (GenBank accession no. AY323810). Spliced variant consists of a 75-bp insertion. *B*: amino acid sequence of rat Ca^2 channel 1C-subunit. Spliced variant contains a 25-amino acid insertion into the I-II cytoplasmic linker that interacts with the -subunit of 1C. *C*: comparison of amino acid sequence of novel 1C-subunit alternatively spliced isoform among several species. Sets of conservative or unconservative residues are indicated in bold or light font, respectively. Amino acid sequence is highly conserved among species.

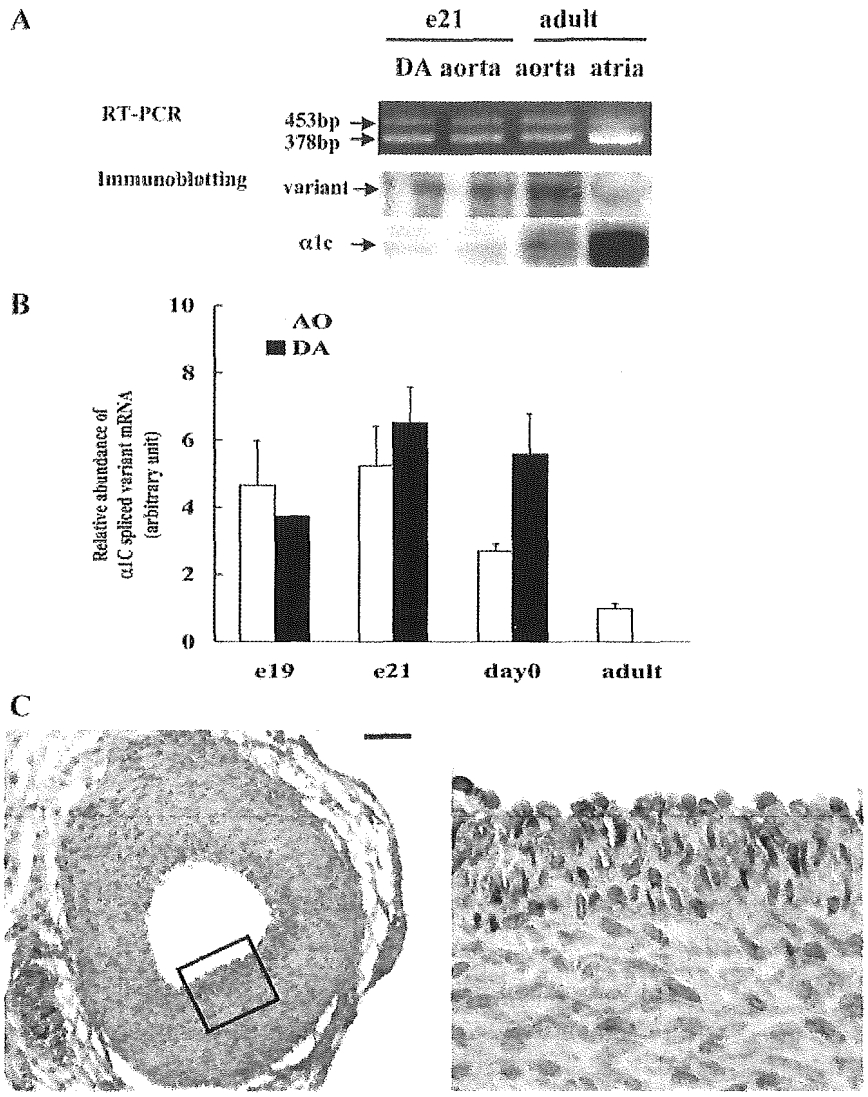

Fig. 7. *A*: expression of splicing variant of $_{1C}$-subunit confirmed by semiquantitative RT-PCR and immunoblotting analyses. Band migrating at 453 bp is spliced variant of $_{1C}$-subunit; smaller band is nonspliced $_{1C}$-isoform. Immunoblotting analysis revealed that spliced variant of $_{1C}$-subunit was highly expressed in vascular smooth muscle, including DA, at mRNA and protein levels. *B*: relative abundance of spliced variant of $_{1C}$-subunit mRNA measured by quantitative RT-PCR. Level of spliced variant of $_{1C}$-subunit mRNA is highly expressed in DA and aorta in the fetus. *C*: immunoreaction of splicing variant of $_{1C}$-subunit was found in smooth muscle cells of DA at e21. Strong immunoreaction was found in region of intimal thickening. Scale bar, 100 m. High-magnification (4) image of region enclosed in rectangle at *left* is shown at *right*.

We examined whether the DA variant exerts any differences in the gating kinetics of the Ca^2 channel. Activation and inactivation kinetics of I_{Ba} were not significantly different between rbCII and the DA variant (Fig. 8*A*). The expression level at the surface membrane, estimated as the density of I_{Ba}, did not differ between the two groups, even though the individual cell showed a wide variety of I_{Ba} density, as is often the case with a transient expression experiment (Fig. 8*B*). The *I-V* relations of rbCII and the DA variant were almost superimposable (Fig. 8*C*). $V_{h\text{-}act}$ of rbCII and the DA variant were 15.4 1.9 mV (n 9) and 14.5 1.2 mV (n 7), respectively (not statistically significant). The steady-state inactivation curves could be slightly shifted toward the depolarized direction in the DA variant, but $V_{h\text{-}inact}$ was not significantly different: 33.3 1.0 mV (n 9) and 31.5 1.7 mV (n 6), respectively.

DISCUSSION

Ca^2 influx through VDCCs plays an important role in vascular myogenic reactivity and tone (4, 8, 26). To our knowledge, the present study demonstrated the first complete characterization of the expression of VDCC subtype mRNAs in the DA. Tristani-Firouzi et al. (38) demonstrated that activation of L-type, but not T-type, VDCCs plays a major role in oxygen-sensitive contraction in the DA. Takizawa et al. (37) demonstrated that an L-type VDCC blocker, verapamil, inhibits its spontaneous closure of the DA in newborn rats. Therefore, the abundant expression of $_{1C}$-subunit mRNA in the DA suggested that the $_{1C}$-subunit is mainly responsible for the influx of Ca^2 that induces contraction of the DA after birth.

We also found that all T-type VDCCs were expressed in the DA. The most dominant isoform among T-type VDCCs in the DA is the $_{1G}$-subunit, with an expression level 25–120 times higher in fetal vessels than in adult aorta, which is consistent with previous reports showing that T-type VDCCs are predominantly expressed in the early stages of differentiation of many embryonic and neonatal tissues (2, 9, 12, 21). The expression of $_{1G}$-subunit mRNA was significantly upregulated by maternal administration of vitamin A. In the DA, $_{1G}$-subunit protein was highly localized in the region of intimal thicken-

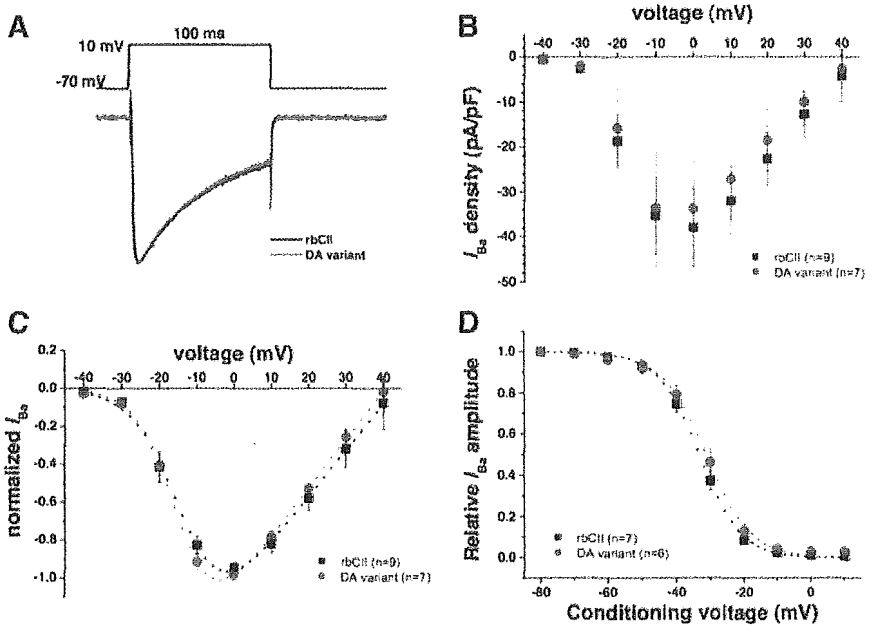

Fig. 8. *A*: Ba^2 current (I_{Ba}) traces of rat brain 1C subunit (rbCII) and the DA variant. Peak normalized currents were averaged and superimposed. Pulse protocol is indicated above current traces. *B*: voltage dependence of I_{Ba} density of DA variant and rbCII. *C*: current-voltage (*I-V*) relations (curve) of rbCII and the DA variant. Amplitude of I_{Ba} was normalized to peak value in each recording and averaged. *D*: steady-state inactivation curves of rbCII and the DA variant. Test pulse to 0 mV for 100 ms was applied after conditioning pulse for 5 s to the respective voltages ranging from 80 to 10 mV in 10-mV steps and for 25 ms at 70 mV. Values are means SE.

ing. Although the abundant expression of the $_{1G}$*-subunit* suggests that the $_{1G}$-subunit plays an important role in the DA, the physiological role of T-type VDCCs in smooth muscle contraction has been obscure. However, Ca^2 influx through the $_{1H}$-subunit has been recently identified to be essential for normal relaxation of coronary arteries (4). Therefore, T-type VDCCs may play a similar role in the DA, rather than in oxygen-sensitive contraction (38). Further investigation is necessary to test the possibility.

In addition to the regulation of vascular tone, L- and T-type VDCCs are also known to regulate differentiation (14, 17), proliferation (19, 36, 44), migration (7, 31), and gene expression (41) in vascular SMCs. In the present study, we found that L- and T-type Ca^2 channel blockers significantly inhibited [^{3}H]thymidine incorporation in DA SMCs, suggesting that L- and T-type VDCCs promote cell proliferation in the DA. Moreover, we found that BAY K 8644, an L-type VDCC activator, increased DA SMC migration in a dose-dependent manner (unpublished data). A previous study demonstrated that the blockade of T-type, but not L-type, VDCCs prevented neointima formation after vascular injury (32), which shares a molecular mechanism of intimal thickening similar to that of the DA. Our present results, however, indicate that L- and T-type VDCCs are involved in intimal thickening in the DA in different ways.

Previous studies demonstrated that responses of the DA to oxygen and indomethacin, a prostaglandin H synthase inhibitor, are blunted at e19 and are apparent at e21 (24, 25). In this study, the expression level of $_{1C}$-subunit mRNA at e19 was similar to that at e21 or *day 0*. Therefore, the expression level of the $_{1C}$-subunit was not considered the cause of the blunted response of the DA to oxygen and indomethacin at e19. One may argue that an oxygen-sensitive signal is activated at near term (e21) to increase the activity of VDCCs. In this sense, vitamin A and/or retinoic acid signaling is a candidate for the activator of oxygen sensitivity, because the retinoic acid response element is strongly expressed in the mouse DA (6), and *maternally administered vitamin A accelerated development of* the oxygen-sensing mechanism of the rat DA (42). Previous studies have also demonstrated that retinoic acid upregulated $_{1C}$-subunit L-type Ca^2 channel expression in vascular SMCs (13) and H_9C_2 cardiac myoblast cell lines (22). Although vitamin A upregulated the expression of $_{1C}$-subunit mRNA in the DA only at *day 0*, it would be of great interest that vitamin A and/or retinoic acid signal may enhance the activity of VDCCs in the DA.

We found a novel spliced variant of the $_{1C}$-subunit in the rat. The spliced variant contained a 25-amino acid insertion into the I-II cytoplasmic linker. The interaction between the cytoplasmic I-II linker of $_{1C}$- and -subunits is known to modulate channel opening (16). During the preparation of this manuscript, Liao et al. (18) reported the same spliced variant of the $_{1C}$-subunit. They demonstrated that the spliced variant of the $_{1C}$-subunit exhibited a hyperpolarized shift in voltage-dependent activation and the *I-V* relation in HEK 293 cells. However, we did not find a difference in basic electrophysiological channel properties between the conventional and the spliced variant of $_{1C}$-subunits. Although we do not explain an exact reason for the conflicting results between two studies, the discrepancy may be due to the different conditions of the experiments: we used rat cDNA and the $_1$-subunit, whereas Liao et al. used human cDNA and the $_2$-subunit. Although we did not find a difference in basic channel properties between the conventional and the spliced variant of $_{1C}$-subunits, we found the distinct expression pattern of the spliced variant in the DA. The spliced variant was strongly expressed in neointimal thickening of the DA, where SMCs exhibit more proliferating and migrating characters (33, 34). In addition, we found that expression of the spliced variant mRNA was significantly increased in the lung of monocrotaline-treated rats (unpublished data). These results suggest a distinct role for the spliced variant in adaptation to various physiological and/or pathological signals.

In conclusion, multiple VDCC subunits were identified in the DA, and, in particular, $_{1C}$- and $_{1G}$-subunits were predominant in the DA. The expression of $_{1C}$- and $_{1G}$-subunit mRNAs was higher in the DA than in the aorta and was significantly upregulated by maternal administration of vitamin A. We found a novel spliced variant of the $_{1C}$-subunit gene that may play a specific role in Ca^2 entry in the lung and fetal arteries. Our study could be an important first step in identification of the molecular basis of Ca^2 channel function in the DA. On the basis of our results, further study would identify the physiological relevance between mRNA levels and Ca^2 channel function in the DA.

ACKNOWLEDGMENTS

We are grateful to Takayo Musuda, Mayumi Watanabe, and Chikako Usami for excellent technical assistance and animal care. Efonidipine was kindly provided by Nissan Chemical Industries (Saitama, Japan).

GRANTS

This work was partly supported by the Mother and Child Health Foundation (S. Minamisawa), 2005 Strategic Research Project Grant K17014 of Yokohama City University (S. Minamisawa), the Yokohama Foundation for Advancement of Medical Science (U. Yokoyama and T. Akaike), and a Grant-in-Aid for Scientific Research from the Japanese Society for the Promotion of Science (S. Adachi-Akahane).

REFERENCES

1. **Arikkath J and Campbell KP.** Auxiliary subunits: essential components of the voltage-gated calcium channel complex. *Curr Opin Neurobiol* 13: 298–307, 2003.
2. **Bijlenga P, Liu JH, Espinos E, Haenggeli CA, Fischer-Lougheed J, Bader CR, and Bernheim L.** T-type $_{1H}$ Ca^2 channels are involved in Ca^2 signaling during terminal differentiation (fusion) of human myoblasts. *Proc Natl Acad Sci USA* 97: 7627–7632, 2000.
3. **Catterall WA.** Structure and regulation of voltage-gated Ca^2 channels. *Annu Rev Cell Dev Biol* 16: 521–555, 2000.
4. **Chen CC, Lamping KG, Nuno DW, Barresi R, Prouty SJ, Lavoie JL, Cribbs LL, England SK, Sigmund CD, Weiss RM, Williamson RA, Hill JA, and Campbell KP.** Abnormal coronary function in mice deficient in $_{1H}$ T-type Ca^2 channels. *Science* 302: 1416–1418, 2003.
5. **Coceani F and Olley PM.** The control of cardiovascular shunts in the fetal and perinatal period. *Can J Physiol Pharmacol* 66: 1129–1134, 1988.
6. **Colbert MC, Kirby ML, and Robbins J.** Endogenous retinoic acid signaling colocalizes with advanced expression of the adult smooth muscle myosin heavy chain isoform during development of the ductus arteriosus. *Circ Res* 78: 790–798, 1996.
7. **Corsini A, Bonfatti M, Quarato P, Accomazzo MR, Raiteri M, Sartani A, Testa R, Nicosia S, Paoletti R, and Fumagalli R.** Effect of the new calcium antagonist lercanidipine and its enantiomers on the migration and proliferation of arterial myocytes. *J Cardiovasc Pharmacol* 28: 687–694, 1996.
8. **Davis MJ and Hill MA.** Signaling mechanisms underlying the vascular myogenic response. *Physiol Rev* 79: 387–423, 1999.
9. **Del Toro R, Levitsky KL, Lopez-Barneo J, and Chiara MD.** Induction of T-type calcium channel gene expression by chronic hypoxia. *J Biol Chem* 278: 22316–22324, 2003.
10. **De Reeder EG, Poelmann RE, van Munsteren JC, Patterson DF, and Gittenberger-de Groot AC.** Ultrastructural and immunohistochemical changes of the extracellular matrix during intimal cushion formation in the ductus arteriosus of the dog. *Atherosclerosis* 79: 29–40, 1989.
11. **Fearon IM, Varadi G, Koch S, Isaacsohn I, Ball SG, and Peers C.** Splice variants reveal the region involved in oxygen sensing by recombinant human L-type Ca^2 channels. *Circ Res* 87: 537–539, 2000.
12. **Ferron L, Capuano V, Deroubaix E, Coulombe A, and Renaud JF.** Functional and molecular characterization of a T-type Ca^2 channel during fetal and postnatal rat heart development. *J Mol Cell Cardiol* 34: 533–546, 2002.
13. **Gollasch M, Haase H, Ried C, Lindschau C, Morano I, Luft FC, and Haller H.** L-type calcium channel expression depends on the differentiated state of vascular smooth muscle cells. *FASEB J* 12: 593–601, 1998.
14. **Gollasch M, Lohn M, Furstenau M, Nelson MT, Luft FC, and Haller H.** Ca^2 channels, "quantized" Ca^2 release, and differentiation of myocytes in the cardiovascular system. *J Hypertens* 18: 989–998, 2000.
15. **Hofmann F, Lacinova L, and Klugbauer N.** Voltage-dependent calcium channels: from structure to function. *Rev Physiol Biochem Pharmacol* 139: 33–87, 1999.
16. **Hohaus A, Poteser M, Romanin C, Klugbauer N, Hofmann F, Morano I, Haase H, and Groschner K.** Modulation of the smooth-muscle L-type Ca^2 channel $_1$ subunit ($_{1C-b}$) by the $_{2a}$ subunit: a peptide which inhibits binding of to the I-II linker of $_1$ induces functional uncoupling. *Biochem J* 348: 657–665, 2000.
17. **Kuga T, Kobayashi S, Hirakawa Y, Kanaide H, and Takeshita A.** Cell cycle-dependent expression of L- and T-type Ca^2 currents in rat aortic smooth muscle cells in primary culture. *Circ Res* 79: 14–19, 1996.
18. **Liao P, Yu D, Lu S, Tang Z, Liang MC, Zeng S, Lin W, and Soong TW.** Smooth muscle-selective alternatively spliced exon generates functional variation in $Ca_v1.2$ calcium channels. *J Biol Chem* 279: 50329–50335, 2004.
19. **Lijnen P, Fagard R, and Petrov V.** Mibefradil-induced inhibition of proliferation of human peripheral blood mononuclear cells. *J Cardiovasc Pharmacol* 33: 595–604, 1999.
20. **McCleskey EW.** Calcium channels: cellular roles and molecular mechanisms. *Curr Opin Neurobiol* 4: 304–312, 1994.
21. **McCobb DP, Best PM, and Beam KG.** Development alters the expression of calcium currents in chick limb motoneurons. *Neuron* 2: 1633–1643, 1989.
22. **Menard C, Pupier S, Mornet D, Kitzmann M, Nargeot J, and Lory P.** Modulation of L-type calcium channel expression during retinoic acid-induced differentiation of H9C2 cardiac cells. *J Biol Chem* 274: 29063–29070, 1999.
23. **Minamisawa S, Oshikawa J, Takeshima H, Hoshijima M, Wang Y, Chien KR, Ishikawa Y, and Matsuoka R.** Junctophilin type 2 is associated with caveolin-3 and is down-regulated in the hypertrophic and dilated cardiomyopathies. *Biochem Biophys Res Commun* 325: 852–856, 2004.
24. **Momma K, Nakanishi T, and Imamura S.** Inhibition of in vivo constriction of fetal ductus arteriosus by endothelin receptor blockade in rats. *Pediatr Res* 53: 479–485, 2003.
25. **Momma K, Toyono M, and Miyagawa-Tomita S.** Accelerated maturation of fetal ductus arteriosus by maternally administered vitamin A in rats. *Pediatr Res* 43: 629–632, 1998.
26. **Moosmang S, Schulla V, Welling A, Feil R, Feil S, Wegener JW, Hofmann F, and Klugbauer N.** Dominant role of smooth muscle L-type calcium channel $Ca_v1.2$ for blood pressure regulation. *EMBO J* 22: 6027–6034, 2003.
27. **Naguro I, Nagao T, and Adachi-Akahane S.** Ser^{1901} of $_{1C}$ subunit is required for the PKA-mediated enhancement of L-type Ca^2 channel currents but not for the negative shift of activation. *FEBS Lett* 489: 87–91, 2001.
28. **Nakanishi T, Gu H, Hagiwara N, and Momma K.** Mechanisms of oxygen-induced contraction of ductus arteriosus isolated from the fetal rabbit. *Circ Res* 72: 1218–1228, 1993.
29. **Plant TD, Schirra C, Katz E, Uchitel OD, and Konnerth A.** Single-cell RT-PCR and functional characterization of Ca^2 channels in motoneurons of the rat facial nucleus. *J Neurosci* 18: 9573–9584, 1998.
30. **Rabinovitch M.** Cell-extracellular matrix interactions in the ductus arteriosus and perinatal pulmonary circulation. *Semin Perinatol* 20: 531–541, 1996.
31. **Ruiz-Torres A, Lozano R, Melon J, and Carraro R.** L-calcium channel blockade induced by diltiazem inhibits proliferation, migration and F-actin membrane rearrangements in human vascular smooth muscle cells stimulated with insulin and IGF-1. *Int J Clin Pharmacol Ther* 41: 386–391, 2003.
32. **Schmitt R, Clozel JP, Iberg N, and Buhler FR.** Mibefradil prevents neointima formation after vascular injury in rats. Possible role of the blockade of the T-type voltage-operated calcium channel. *Arterioscler Thromb Vasc Biol* 15: 1161–1165, 1995.
33. **Slomp J, Gittenberger-de Groot AC, Glukhova MA, Conny van Munsteren J, Kockx MM, Schwartz SM, and Koteliansky VE.** Differentiation, dedifferentiation, and apoptosis of smooth muscle cells during the development of the human ductus arteriosus. *Arterioscler Thromb Vasc Biol* 17: 1003–1009, 1997.
34. **Slomp J, Gittenberger-de Groot AC, Koteliansky VE, Glukhova MA, Bogers AJ, and Poelmann RE.** Cytokeratin expression in human arteries

pertinent to intimal thickening formation in the ductus arteriosus. *Differentiation* 61: 305–311, 1997.

35. **Snutch TP, Tomlinson WJ, Leonard JP, and Gilbert MM.** Distinct calcium channels are generated by alternative splicing and are differentially expressed in the mammalian CNS. *Neuron* 7: 45–57, 1991.
36. **Sperti G and Colucci WS.** Calcium influx modulates DNA synthesis and proliferation in A7r5 vascular smooth muscle cells. *Eur J Pharmacol* 206: 279–284, 1991.
37. **Takizawa T, Oda T, Arishima K, Yamamoto M, Masaoka T, Somiya H, Akahori F, and Shiota K.** A calcium channel blocker verapamil inhibits the spontaneous closure of the ductus arteriosus in newborn rats. *J Toxicol Sci* 19: 171–174, 1994.
38. **Tristani-Firouzi M, Reeve HL, Tolarova S, Weir EK, and Archer SL.** Oxygen-induced constriction of rabbit ductus arteriosus occurs via inhibition of a 4-aminopyridine-, voltage-sensitive potassium channel. *J Clin Invest* 98: 1959–1965, 1996.
39. **Tsien RW, Lipscombe D, Madison DV, Bley KR, and Fox AP.** Multiple types of neuronal calcium channels and their selective modulation. *Trends Neurosci* 11: 431–438, 1988.
40. **Uemura N, Ohkusa T, Hamano K, Nakagome M, Hori H, Shimizu M, Matsuzaki M, Mochizuki S, Minamisawa S, and Ishikawa Y.** Down-regulation of sarcolipin mRNA expression in chronic atrial fibrillation. *Eur J Clin Invest* 34: 723–730, 2004.
41. **Wamhoff BR, Bowles DK, McDonald OG, Sinha S, Somlyo AP, Somlyo AV, and Owens GK.** L-type voltage-gated Ca^2 channels modulate expression of smooth muscle differentiation marker genes via a Rho kinase/myocardin/SRF-dependent mechanism. *Circ Res* 95: 406–414, 2004.
42. **Wu GR, Jing S, Momma K, and Nakanishi T.** The effect of vitamin A on contraction of the ductus arteriosus in fetal rat. *Pediatr Res* 49: 747–754, 2001.
43. **Yamaguchi S, Okamura Y, Nagao T, and Adachi-Akahane S.** Serine residue in the IIIS5-S6 linker of the L-type Ca^2 channel $_{1C}$ subunit is the critical determinant of the action of dihydropyridine Ca^2 channel agonists. *J Biol Chem* 275: 41504–41511, 2000.
44. **Yang Z, Noll G, and Luscher TF.** Calcium antagonists differently inhibit proliferation of human coronary smooth muscle cells in response to pulsatile stretch and platelet-derived growth factor. *Circulation* 88: 832–836, 1993.